Journal of Bioresources and Bioproducts 6 (2021) 160–167

Contents lists available at ScienceDirect

Journal of Bioresources and Bioproducts

journal homepage: http://www.keaipublishing.com/en/journals/Journal of Bioresources and Bioproducts/

Experimental evaluation of rice husk ash for applications in geopolymer mortars

G. Ogwang [a], P.W. Olupot [a,*], H. Kasedde [a], E. Menya [b], H. Storz [c], Y. Kiros [d]

[a] Department of Mechanical Engineering, College of Engineering, Design, Art and Technology, Makerere University, P.O. Box 7062, Kampala-Uganda
[b] Department of Biosystems Engineering, Gulu University, P.O. Box 166, Gulu, Uganda
[c] Thuenen Institute of Agricultural Technology, Bundesallee 47, 38116 Braunschweig, Germany
[d] Department of Chemical Engineering, KTH Royal Institute of Technology, SE 100 44 Stockholm, Sweden

ARTICLE INFO

Keywords:
Rice husk ash
Metakaolin
Activator
Geopolymer mortar
Characterization

ABSTRACT

Rice husks obtained from upland and lowland rice varieties were characterized for composition and content of ash. Each of the rice husk varieties was fired at temperatures of 600, 800 and 900 °C for a soaking period of 3 h. The resultant rice husk ash was analyzed for oxide composition and crystallinity using X-ray fluorescence and diffraction techniques, respectively. The generated amorphous ash with the highest silica content, together with metakaolin, aggregate, water, and an alkaline activator was employed to formulate geo-polymer mortar prisms according to the standard EN 196–1. Results showed that the content of ash in the varieties ranged from 18.3% to 28.6% dry basis. Out of this, 89 wt%–96 wt% was silica, with amorphous and crystalline forms of silica obtained at 600 °C and 900 °C, respectively, regardless of the rice variety. However, at 800 °C, the silica in the generated ash exhibited both amorphous and crystalline forms. The amorphous ash generated at 600 °C was used in formulation of geopolymer mortars. Compressive and flexural strength of the formulated mortar after 7 days of curing was 1.5 and 1.3 MPa, respectively. These results reveal the firing protocol to form pozzolanic ash, with potential applications in mortar production.

1. Introduction

The increasing demand for cement in the construction sector has accelerated the exploitation of the few available limestone reserves, alongside increased CO_2 emissions, which account for 8% of the global anthropogenic CO_2 emissions (Singh, 2018). These emissions result from the calcination of limestone (Singh et al., 2015), combustion of fossil fuels to maintain high temperatures in the kiln (Zhang et al., 2014), and from electricity use during the grinding of raw and finished materials (Bosoaga et al., 2009). Because of the negative environmental impacts associated with cement production, there is a need to find sustainable options capable of reducing the carbon footprint of the cement industry. For instance, 1) through energy efficiency improvement, 2) waste heat recovery, 3) carbon capture and storage, 4) fossil fuel substitution with renewable energy, and 5) through production of low-carbon cement achieved by replacing the ordinary Portland cement (OPC) with alternative materials, such as blast furnace slag, coal fly ash, natural pozzolanic materials, or geo-polymer (Maddalena et al., 2018).

Among the low-carbon cements, geo-polymer offers better prospects for using as an alternative to OPC, due to its early compressive strength, low permeability, good chemical resistance, as well as due to its excellent fire resistance behavior (Singh et al., 2015). Aside

* Corresponding author: Department of Mechanical Engineering, College of Engineering, Design, Art and Technology, Makerere University, P.O. Box 7062, Kampala-Uganda.
E-mail address: polupot@cedat.mak.ac.ug (P.W. Olupot).

https://doi.org/10.1016/j.jobab.2021.02.008
Received 19 June 2020; Received in revised form 25 August 2020; Accepted 1 September 2020
Available online 26 February 2021

Table 1
Rice varieties and their geographical origin in Uganda.

Geographical origin	Rice variety
Doho Irrigation Scheme, Butalejja District	K98
Kibimba Irrigation Scheme, Bugiri District	Pusa 9
Ngetta Zonal Agricultural Research and Development Institute, Lira District	NERICA 4 and 10

Note: NERICA implies New Rice for Africa.

from that, the OPC replacement with geo-polymer paves way for disposing off agricultural wastes, especially in the developing countries, where sustainable disposal still remains a huge challenge (Menya et al., 2018). For instance, instead of open dumping and/or burning, rice husks can be combusted under controlled conditions to generate rice husk ash with a high silica content (80%–90%) (Menya et al., 2020), as well as with properties desired in geo-polymer production (Detphan and Chindaprasirt, 2009). More specifically, by combusting rice husks at temperatures below 700 ˚C and above 800 ˚C, the amorphous and crystalline forms of ash are obtained, respectively (Fernandes et al., 2016). The crystalline form is less reactive, while the amorphous form exhibits active pozzolanicity under normal conditions (Nair et al., 2008). Therefore, for purposes of producing geo-polymer cement, the amorphous form of the rice husk ash is more suited, as compared with its crystalline counterpart (Fernandes et al., 2016). Moreover, compared with other silica sources like sand, bentonite, and diatomaceous earth, rice husk ash exhibits minimal amounts of contaminants which otherwise affect its performance in applications, where high purity of the ash is required.

Geo-polymer is synthesized through alkali activation of source materials rich in silica and alumina, forming an inorganic alumino–silicate polymer product with polymeric Si–O–Al–O bonds (Daniel et al., 2017). Alumina can be sourced from metakaolin obtained from the calcination of kaolin at a temperature of about 750 ˚C. Metakaolin exhibits high pozzolanic reactivity and filling effects, responsible for the enhanced mechanical properties and durability of geo-polymer (Nuaklong et al., 2018). The alkaline activators include sodium hydroxide (NaOH), potassium hydroxide (KOH), sodium silicate (Na_2SiO_3) and potassium silicate (K_2SiO_3) (Singh et al., 2015). Rice husk ash has been previously employed in combination with different alumina source materials to produce geo-polymer. For instance, rice husk ash and red mud (He et al., 2013), rice husk ash and fly ash (Hwang and Huynh, 2015), rice husk ash and metakaolin (Sore et al., 2016). This study aimed at characterization of rice husk ash from the rice varieties predominantly grown in Uganda, alongside other alumino-silicates for production of geo-polymer cement. The resultant rice husk ash (RHA) was analyzed for oxide composition and for crystallinity by employing X-ray fluorescence (XRF) and X-ray diffraction (XRD) techniques, respectively. The selected rice husk ash, together with metakaolin, aggregate, water and an alkaline activator was employed to formulate geo-polymer mortar prisms according to the standard BS EN 196–1 (Methods of Testing Cement-Part 1: Determination of Strength, Brussels, 2005). This work contributes to the characterization of renewable biomass and the conversion of renewable bioresources into biomaterials.

2. Materials and methods

2.1. Sample collection and preparation

2.1.1. Rice husk

Four rice varieties predominantly grown in Uganda were obtained from selected Irrigation Schemes (lowland rice varieties) and from Ngetta Zonal Agricultural Research and Development Institute (upland rice varieties) as indicated in Table 1. Rice agronomists were involved to identify the rice varieties. To obtain the rice husks, 60 kg of each of the rice varieties, dried to moisture content of 13%–14% wet basis (wb) were identically milled using a milltop rice milling machine (Model SB-10). The generated rice husk samples were water-washed and subsequently sun dried for 5 h, prior to incineration.

2.1.2. Rice husk ash and metakaolin

Rice husk ash was produced from each of the four generated rice husk varieties, by firing the husks in a kiln at temperatures of 600, 800 and 900 ˚C, for a soaking period of 3 h. The temperature was regulated by carefully controlling the quantity of firewood present in the combustion chamber. The temperature was monitored by using a pyrometer (RT Series). At the end of each experimental run, the kiln was allowed to cool to ambient conditions, prior to the rice husk ash removal.

The kaolin employed in this study was sourced from Mutaka in the Bushenyi District in Uganda. Metakaolin was obtained by calcination of the kaolin in an electric furnace at a heating rate of 20 ˚C/min from 25 ˚C to 750 ˚C for 2 h. The as-mined sample was allowed to cool to room temperature, prior to its removal from the furnace for subsequent wet milling, sieving (45 μm sieve), and drying. A total of 2 kg of metakaolin was prepared for the study.

2.1.3. Alkaline activators and fine aggregate

The alkaline activators included NaOH and sodium silicate (Na_2SiO_3). The 10 mol/L and 500 g of NaOH and Na_2SiO_3, respectively, were procured from the Perkins Laboratory Stores in Kampala, Uganda. These two activators were preferred, since their mixture produces materials with higher mechanical strength than what is possible with either of the activators.

The fine aggregate was sourced from the Materials Laboratory of Uganda's Ministry of Works and Transport. This was subsequently prepared according to Euro code, EN 196 Part 1: 2016 Code Test Specification for Cement Properties.

Table 2
Compositions of formulated geopolymer cement by weight (wt).

Composition	Value
RHA (g)	180
Metakaolin (g)	420
Na_2SiO_3 (g)	200
NaOH (g)	100
Aggregates (sand) (g)	1350
Water (mL)	450

Note: RHA, rice husk ash.

2.2. Characterization

2.2.1. Rice husk

(1) Bulk density. The bulk density of rice husk was determined according to the American Society for Testing and Materials (ASTM) E873–82 (ASTM, 2013). According to this procedure, the rice husk samples were loosely filled in a cylindrical container of mass, 16.08 g and volume, 200 cm^3 (diameter 5.80 cm, height 7.57 cm), followed by measuring the weight using a weighing balance (Model: KERN GS). The net weight was then determined as the difference between the total weight of the cylindrical container with the sample and weight of the empty cylindrical container. The bulk density of the rice husks was then determined as the ratio of mass of sample to the volume of the cylindrical container.

(2) Proximate analysis. The proximate composition of the rice husks was obtained by employing thermogravimetric analysis. Approximately 15 mg sample of each rice husk variety sieved to size 0.25 μm was heated in a thermal analyzer (TA instruments Q500). The weight was lost as a result of heating the rice husk sample at a heating rate of 20 °C/min from 25 °C to 105 °C in nitrogen (60 mL/min) until constant weight was achieved as the moisture content in the rice husk. Volatile matter was obtained as weight loss resulting from heating the oven dried rice husk sample in nitrogen at a heating rate of 20 °C/min from 25 °C to 900 °C, and holding at the final temperature until constant weight was achieved. Additional weight loss occurred when the residual char was combusted in air (60 mL/min) at a temperature of (575 ± 25) °C. This weight loss is due to the combustion of the remaining organic material which is the fixed carbon content. Further, the inorganic residue obtained after combustion of the residual char gives the ash content.

(3) Ultimate analysis. Ultimate analysis was carried out to determine the elemental composition of the rice husks, such as carbon (C), hydrogen (H), sulfur (S), nitrogen (N), and oxygen (O). The C, H, and S were determined using an ELTRA CHS analyzer, while nitrogen was determined using the Kjeldahl method (AACC International, 2000). This is based on the conversion of the fuel bound nitrogen to ammonia (NH_3), which is subsequently separated by distillation and determined by titration using HCl solution and methyl red as an indicator.

2.2.2. Rice husk ash analyses

The resultant RHA was analyzed for oxide composition, as well as for crystallinity by employing XRF and XRD, respectively.

2.3. Preparation of geo-polymer mortar

The amorphous rice husk ash, generated from firing the rice husks at 600 °C, with the highest silica content, together with the metakaolin, aggregate, water and an alkaline activator were employed to formulate the geo-polymer mortar prisms according to the standard BS EN 196–1 (2005). The formulation was made to obtain the ratio of Na_2SiO_3 to NaOH as 2 (Bakri et al., 2012), the weight of the RHA as 30% of metakaolin (Borges et al., 2016), and the ratio of fine aggregate to combination of RHA and metakaolin as 2 (Saloma et al., 2017) (Table 2).

The RHA and metakaolin were initially mixed, followed by addition of an alkaline activator solution, forming geo-polymer cement. The alkaline activator solution was prepared by mixing liquid sodium hydroxide with solid sodium silicate. Once the geo-polymer cement was formulated, fine aggregates (sand) together with distilled were subsequently added to the cement according to the mix proportions shown in Table 2. The resultant mixture was subjected to mixing in an automatic laboratory mixer for 5 min. The formed material was transferred to prismatic moulds, which were subsequently placed in an automatic vibrator for about 4 min to ensure an equal distribution of the mix in the prisms. The prisms were then allowed to cure at room temperature for 7 days. In total, six test mortar prisms of 160 mm × 40 mm × 40 mm were made as shown in Fig. 1.

2.4. Strength characteristics

Both tests of flexural and compressive strength were carried out on the formulated geopolymer mortar. Flexural strength was determined using the three-points loading method with an automatic flexural tensile tester L15 machine as per the EN196–1: 2010

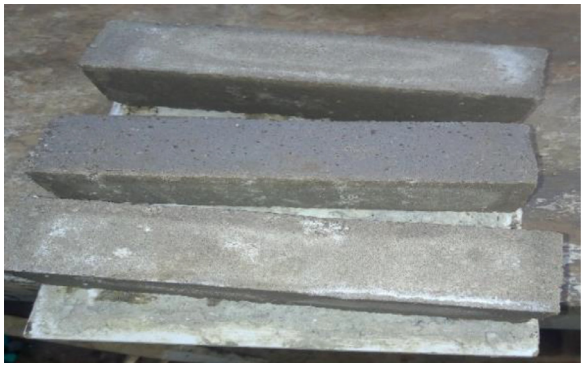

Fig. 1. Prisms of geo-polymer mortar produced.

Table 3
Proximate and ultimate properties of rice husk varieties in Uganda.

Rice variety	Ultimate analysis (%, dry ash free basis)					Proximate analysis (%, dry basis)			BD (kg/m^3)	MC (wt%)
	C	H	S	N	O	Ash	FC	VM		
NERICA 10	35.61	6.05	0.01	0.81	57.52	18.33	18.68	62.99	102.85	7.34
NERICA 4	33.86	5.82	0.21	0.81	59.31	18.94	18.25	62.81	105.98	7.39
K-98	33.01	5.34	0.07	0.82	60.77	27.34	15.90	56.76	134.27	7.50
Pusa	30.67	4.90	0.15	0.58	63.71	28.58	15.69	55.73	124.82	7.35

Notes: FC, fixed carbon; VM, volatile matter; BD, bulk density; MC, moisture content; and wt, wet basis.

method. The samples were each put in the testing machine with one side face on the supporting rollers and with the longitudinal axis normal to the supports. The loads were then applied vertically by means of the loading rollers to the opposite side face of the prism/or samples and the load increased smoothly at a rate of 50 N/s until the specimen fractured. The broken prism/samples halves were kept and then used for the compressive strength test. The final flexural strength result was as a result of arithmetic mean of the values of three test samples.

The compressive strength test was carried out by using an electronically operated wizard basic compression test machine on broken specimens from the flexural strength test experiments. The test samples were placed in the hydraulic testing frame and a force was applied until the specimen broke. The prism halves were centered laterally to the platens of the machine within ±0.5 mm and longitudinally so that the end face of the prism overhangs the platens by about 10 mm. The maximum force applied and the dimensions of the specimen were then recorded and compressive strength calculated. The final compressive strength results were as a result of arithmetic mean of the values of six individual test samples. Early strength of a cement is the compressive strength determined in accordance with the Uganda Standard, US99/EAS 148–1 (2017, Cement Test Methods Part 1. Determination of Strength. Uganda National Bureau of Standards, Kampala. Uganda) after 7 days.

3. Results and discussion

3.1. Characterization

3.1.1. Proximate and ultimate composition

The results from the proximate and ultimate analyses of the raw rice husk varieties on dry basis are shown in Table 3. From the Table, the volatile matter, fixed carbon, and ash content of the rice husk varieties ranged from 55.73–62.99, 15.69–18.68, and from 18 to 8.58% dry basis, respectively. The upland varieties show typically low ash contents as compared with the lowland varieties. This result is expected since rainwater, a product of distillation and usually the only source of water for upland rice lacks silicon element, which otherwise accounts for 90 wt%–98 wt% composition of ash (Mansaray and Ghaly, 1997; Length, 2009).

With the exception of the oxygen content, the remaining composition parameters of the rice husk varieties shown in Table 3 are close to those of rice husks published elsewhere (Kumagai et al., 2007; Alvarez et al., 2015; Liu et al., 2016). Similar to upland rice husk varieties, the variation in the ultimate composition of lowland rice husk varieties was minimal. The average nitrogen content of upland rice husk varieties (0.81% dry basis) was generally higher than that of lowland rice husk varieties (0.7% dry basis). This is expected, since the major limiting nutrient for lowland paddy rice production is nitrogen (Wanyama et al., 2015). However, the generally low nitrogen and sulfur contents in both lowland and upland rice husk varieties are of environmental benefit, since upon thermochemical treatment of rice husks, a minimal risk of NO_x and SO_x emissions could be expected (Tripathi et al., 2016).

Table 4
The X-ray fluorescence (XRF) results for RHA and kaolin.

Sample ID	T (˚C)*	SiO_2	Al_2O_3	Fe_2O_3	CaO	MgO	SO_3	K_2O	Na_2O	Ti_2O_3	P_2O_5	Mn_2O_3	LOI
K 98	600	94.91	0.37	0.79	0.98	0.26	0.09	1.67	0.02	0.11	0.56	0.18	0.06
K 98	800	95.63	0.32	0.69	0.75	0.25	0.07	1.44	0.04	0.09	0.54	0.17	0.02
K 98	900	95.65	0.30	0.72	0.77	0.26	0.05	1.48	0.02	0.08	0.50	0.16	0.00
PUSA 9	600	94.50	0.43	0.86	1.02	0.16	0.21	2.19	0.00	0.13	0.32	0.12	0.05
PUSA 9	800	94.86	0.37	0.89	1.00	0.21	0.17	1.77	0.18	0.11	0.31	0.12	0.01
PUSA 9	900	93.81	0.29	1.87	1.04	0.18	0.20	1.85	0.17	0.12	0.32	0.13	0.02
NERICA 10	600	89.57	0.85	1.12	1.57	0.57	0.09	5.48	0.00	0.21	0.39	0.11	0.04
NERICA 10	800	89.45	0.92	1.26	1.85	0.57	0.08	5.11	0.00	0.23	0.39	0.13	0.02
NERICA 10	900	89.07	0.99	1.38	2.07	0.63	0.27	4.73	0.12	0.23	0.36	0.14	0.02
NERICA 4	600	91.38	0.72	0.97	1.68	0.51	0.12	3.79	0.00	0.16	0.52	0.09	0.05
NERICA 4	800	90.61	0.90	1.33	2.08	0.41	0.06	3.66	0.00	0.23	0.53	0.13	0.05
NERICA 4	900	89.65	0.83	2.28	2.02	0.33	0.14	3.81	0.00	0.26	0.51	0.15	0.03
Kaolin	–	55.78	29.42	0.68	0.55	0.21	0.00	2.22	0.02	0.08	0.01	0.02	11.02

Notes: * implies temperature, and LOI implies loss on ignition.

3.1.2. Bulk density and moisture

The results in Table 3 indicate that the mean bulk density of upland rice husk varieties (NERICA 10 and NERICA 4) is typically lower than that of lowland rice husk varieties (K-98 and Pusa), with values ranging from 102 to 5.98 kg/m^3 and 124.82–134.27 kg/m^3, respectively. The bulk densities are within the range of 100–400 kg/m^3 reported by Sridhar et al. (1996) for the rice husk from India, higher than the values of 82.98–92.77 kg/m^3 reported by Tirawanichakul et al. (2008) for the rice husk from Thailand.

From Table 3, the moisture content of the rice husk varieties ranged from 7.34 wt%–7.50 wt%. These values are lower than the value of 8.1% reported by Subramanian et al. (2011) for the rice husk from India, the value of 9.8% reported by Vélez et al. (2009) for the rice husk from Colombia, and the values of 8.68%–10.44% reported by Mansaray and Ghaly (1997) for the rice husks from Louisiana (USA) and Sierra Leone. They are, however, higher than the value of 4.2% reported by Kalderis et al. (2008) for the rice husk from India. Bulk density and moisture content of rice husk have shown that the key values are not extreme and hence can be explored for use for various engineering applications as reported in the literature, including use in the formulation of geo-polymer cement and porcelain tiles.

3.1.3. Oxide composition

The results from the XRF analyses of RHA and kaolin are shown in Table 4. The results indicate that, at the firing temperatures considered in this study, the silica content of the rice husk ash ranges from 89 to 5.65%. This is close/or within the range reported by Hossain et al. (2018). The results also indicate that SiO_2 and K_2O are the dominant oxides in the RHA, which is in agreement with findings reported by Jenkins et al. (1998). The lowland rice husk varieties exhibited a higher silica content (93.81%–95.65%), as compared with its upland counterparts (89.07%–91.38%), suggesting that low land rice varieties are better sources of silica than upland rice. The maximum loss on ignition for the rice husk ash was found to be 0.06%, which is lower than the maximum value of 12% required for pozzolanas. This lower value suggests that the RHA contains minimal amounts of unburnt carbon, which would otherwise reduce the pozzolanic activity of the ash. The content of magnesium oxide ranged from 0.16% to 0.63%, which satisfies the required value of 4% maximum for pozzolanas. The total percentage compositions of iron oxide, silicon dioxide and aluminum oxide were found to be ranging from 90.66% to 98.92%. This value is within the required value of 70% minimum for pozzolanas as per American Standard ASTM C 618–78, and as such the rice husk ash is pozzolanic. This pozzolanic nature of the RHA qualifies them to be used as ingredients for making geopolymer cement.

From Table 4, the quality of the kaolin sample compares well with kaolin marketed elsewhere (Kirabira et al., 2005). Kaolin with lower than 1% Fe_2O_3 and Al_2O_3> 29%, is considered to be a good source of metakaolin upon calcination. Overall, the high silica content in the rice husk ash paves way for reducing the need for silica obtained from polluting sources.

3.1.4. Phase analysis of RHA

Fig. 2 shows the XRD patterns of the RHA samples at temperature ranges necessary for the formation of amorphous and crystalline structures. From Fig. 2, it can be deduced that; 1) all the samples at 600 ˚C have amorphous silica, 2) at 800 ˚C onwards, sharp peak of tridymite and cristobalite appear, and 3) at 900 ˚C, crystalline polymorphs like α-cristobalite, α-quartz and α-tridymite are formed. It can also be seen from Fig. 2, that as the temperature increased, improvement in crystallinity was achieved. The sample combusted at 900 ˚C exhibited the utmost crystallinity among the four combusted samples. This is in agreement with findings by Joseph et al. (1989) and Sugita (1993) who reported that amorphous ash is formed at incineration temperatures of 550–800 ˚C, while changes occur from amorphous to crystallinity at temperatures ranging from 800 ˚C to 900 ˚C. Moreover, other studies reported that RHA produced below 700 ˚C would be in an amorphous form, while that above 800 ˚C would exhibit the crystalline form (Mehta, 1979; Maeda et al., 2001).

The amorphous form of silica is composed of silica tetrahedral arranged in a random three dimensional network without regular lattice structures (Muthadhi, 2010). As result of the disordered arrangement, the structure is open with holes in the network where electrical neutrality is not satisfied and the specific surface area is also large. This enhances the reactivity, since a large area is

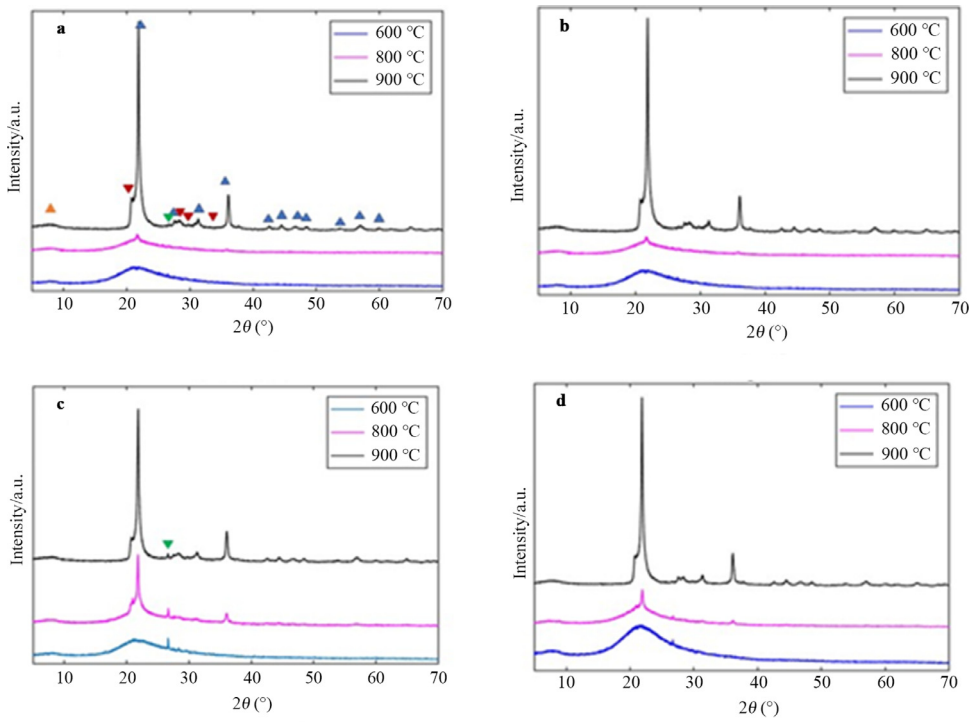

Fig. 2. The X-ray diffraction (XRD) results for RHA from rice husk variety (a) K98, (b) NERICA 4, (c) NERICA 10, and (d) Pusa.

available for reactions to take place. This is therefore suitable for pozzalanic materials, and hence can be used to make geo-polymer cement. Based on these results, the RHA produced at 600 ^{C} was employed as an ingredient from production of geo-polymer cement.

3.2. Strength characteristics

The average compressive and flexural strengths were obtained as 1.45 and 1.28 MPa, respectively. Although these are comparable with results obtained from studies conducted elsewhere (Nath and Sarker, 2012; Al-Majidi et al., 2016; Livi and Repette, 2017), the results are lower than 16 MPa required of cement strength class C32.5 N (UNBS, 2018). According to European Standard EN 197–1: 2011 (Cement-Part 1: Composition, specifications and conformity criteria for common cements. European Committee for Standardization Accessed on September 27, 2020), the compressive strength of OPC at 7 days of curing is ≥ 16 MPa, while for blast furnace cements ≥ 12 MPa. The marked difference between the strengths of OPC and RHA based geopolymers could lie in the difference between their bonds. The principal binding phase of RHA geopolymer cement is Na_n–(–Si–O–Al–O–)$_n$–. However, C–S–H (calcium silicate hydrate) is the principal binding phase of OPC and is responsible for its strength. The C–S–H forms upon hydration of OPC and is the most voluminous hydration phase. The average Ca/Si ratio of OPC is 1.75 (Feng et al., 2013). Therefore, another cation for example Ca^{2+} species from calcium sulfate would be needed to balance the covalent bonding that would make it possible to introduce the strong C–S–H bond into the geopolymer system. The presence of calcium sulfate in the geopolymer may therefore make it stronger as observed by Kusbiantoro et al. (2012). Zareei et al. (2017) reported a positive relationship between 15% replacement of RHA with increase in compressive strengths of OPC by about 20%. This however, was not investigated in this work.

The color of the produced geopolymer mortar prisms/or moulds was darker on the surface (Fig. 1), suggesting employment of RHA in the mixes (Borges et al., 2016). It was possible to observe the formation of efflorescence at the top surface of the samples due to surface carbonation. This carbonation may present limitations on the applicability of geo-polymers, especially as a finishing material. In spite of the surface carbonation, no surface cracking was observed in any of the formulated geo-polymer mortar.

4. Conclusions

The XRF analysis of the RHA showed that its silica content ranges from 89.07 wt% to 95.65 wt%. A 95% silica powder can be produced in amorphous and crystalline form up calcination of the rice husks at 600 and 900 °C, respectively, for 3 h. With such composition, the RHA serves as a potential replacement of silica sources for various engineering applications. The XRD analysis of the RHA showed that the transition temperature from amorphous to crystalline structure ranged from 600 °C and 900 °C, for the rice husk varieties employed in this study. The compressive and flexural strengths of the formulated geo-polymer mortar after 7 days of curing were obtained as 1.45 and 1.28 MPa, respectively. Although these are comparable with results obtained from studies conducted

elsewhere, the results are lower than 16 MPa required of cement strength class C32.5 N. Overall, if employed in combination with metakaolin and alkaline activator, the RHA from the investigated rice varieties offers a very promising ingredient for production of geo-polymer mortar at room temperature.

Declaration of Competing Interest

There is no conflict to declare.

Acknowledgement

The authors gratefully acknowledge funding from the Volkswagen Foundation Germany under the Postdoctoral Fellowships for African Researchers in the Engineering Sciences to Dr. Peter Wilberforce Olupot (Grant No. 90014).

References

A.A.C.C. International, 2000. Approved Methods of the American Association of Cereal Chemists, 10th ed. The Association, St. Paul, MN, USA.
Al-Majidi, M.H., Lampropoulos, A., Cundy, A., Meikle, S., 2016. Development of geopolymer mortar under ambient temperature for *in situ* applications. Constr. Build. Mater. 120, 198–211.
Alvarez, J., Lopez, G., Amutio, M., Bilbao, J., Olazar, M., 2015. Physical activation of rice husk pyrolysis char for the production of high surface area activated carbons. Ind. Eng. Chem. Res. 54, 7241–7250.
ASTM, 2013. American Society for Testing and Materials (ASTM) E873-82. Standard Test Method for Bulk Density of Densified Particulate Biomass Fuels.
Bakri, A.M.M., Kamarudin, H., Bnhussain, M., Nizar, I.K., Rafiza, A.R., Zarina, Y., 2012. The processing, characterization, and properties of fly ash based geopolymer concrete. Rev. Adv. Mater. Sci. 30, 90–97.
Borges, P.H.R., Nunes, V.A., Panzera, T.H., Schileo, G., Feteira, A., 2016. The influence of rice husk ash addition on the properties of metakaolin-based geopolymers. Open Constr. Build. Technol. J. 10, 406–417.
Bosoaga, A., Masek, O., Oakey, J.E., 2009. CO_2 capture technologies for cement industry. Energy Procedia 1, 133–140.
Daniel, A.J., Sivakamasundari, S., Abhilash, D., 2017. Comparative study on the behaviour of geopolymer concrete with hybrid fibers under static cyclic loading. Procedia Eng. 173, 417–423.
Detphan, S., Chindaprasirt, P., 2009. Preparation of fly ash and rice husk ash geopolymer. Int. J. Miner., Metall. Mater. 16, 720–726.
Feng, D.C., Xie, N., Gong, C.W., Leng, Z., Xiao, H.G., Li, H., Shi, X.M., 2013. Portland cement paste modified by TiO_2 nanoparticles: a microstructure perspective. Ind. Eng. Chem. Res. 52, 11575–11582.
Fernandes, I.J., Calheiro, D., Kieling, A.G., Moraes, C.A.M., Rocha, T.L.A.C., Brehm, F.A., Modolo, R.C.E., 2016. Characterization of rice husk ash produced using different biomass combustion techniques for energy. Fuel 165, 351–359.
He, J., Jie, Y.X., Zhang, J.H., Yu, Y.Z., Zhang, G.P., 2013. Synthesis and characterization of red mud and rice husk ash-based geopolymer composites. Cem. Concr. Compos. 37, 108–118.
Hossain, S.S., Mathur, L., Roy, P.K., 2018. Rice husk/rice husk ash as an alternative source of silica in ceramics: a review. J. Asian Ceram. Soc. 6, 299–313.
Hwang, C.L., Huynh, T.P., 2015. Effect of alkali-activator and rice husk ash content on strength development of fly ash and residual rice husk ash-based geopolymers. Constr. Build. Mater. 101, 1–9.
Jenkins, B.M., Baxter, L.L., Miles Jr, T.R., Miles Jr, T.R., 1998. Combustion properties of biomass. Fuel Process. Technol. 54, 17–46.
Joseph, S., Baweja, D., Crookham, G., Cook, D., 1989. Production and utilization of rice husk Sugita. (n.d.).ash preliminary investigations. In: Third CANMET/ACI International Conference on Fly Ash, Silica Fume, Slag and Natural Pozzolans, pp. 861–878.
Kalderis, D., Bethanis, S., Paraskeva, P., Diamadopoulos, E., 2008. Production of activated carbon from bagasse and rice husk by a single-stage chemical activation method at low retention times. Bioresour. Technol. 99, 6809–6816.
Kirabira, J.B., Jonsson, S., Byaruhanga, J.K., 2005. Powder characterization of high temperature ceramic raw materials in the Lake Victoria Region. Silic. Ind. 70, 127–134.
Kumagai, S., Noguchi, Y., Kurimoto, Y., Takeda, K., 2007. Oil adsorbent produced by the carbonization of rice husks. Waste Manag 27, 554–561.
Kusbiantoro, A., Nuruddin, M.F., Shafiq, N., Qazi, S.A., 2012. The effect of microwave incinerated rice husk ash on the compressive and bond strength of fly ash based geopolymer concrete. Constr. Build. Mater. 36, 695–703.
Length, F., 2009. Elemental analysis of rice husk ash using X-ray fluorescence technique. Int. J. Phys. Sci. 4, 189–193.
Liu, B., Gu, J., Zhou, J.B., 2016. High surface area rice husk-based activated carbon prepared by chemical activation with $ZnCl_2$-$CuCl_2$ composite activator. Environ. Prog. Sustain. Energy 35, 133–140.
Livi, C.N., Repette, W.L., 2017. Effect of NaOH concentration and curing regime on geopolymer. Rev. IBRACON Estrut. Mater. 10, 1174–1181.
Maddalena, R., Roberts, J.J., Hamilton, A., 2018. Can Portland cement be replaced by low-carbon alternative materials? A study on the thermal properties and carbon emissions of innovative cements. J. Clean. Prod. 186, 933–942.
Maeda, N., Wada, I., Kawakami, M., Ueda Tand Pushpalal, G., 2001. Development of a new furnace for the production of rice husk ash. In: Proceedings of 7th CANMET/ACI International Conference on Fly Ash, Silica Fume, Slag and Natural Pozzolans in Concrete, Chennai, pp. 835–852.
Mansaray, K.G., Ghaly, A.E., 1997. Physical and thermochemical properties of rice husk. Energy Sources 19, 989–1004.
Mehta, P., 1979. The chemistry and technology of cement made from rice husk ash. In: Proceedings of UNIDO/ESCAP/RCTT Workshop on Rice Husk Ash Cements. Peshawar. Regional Centre for Technology Transfer, Bangalore, pp. 113–122.
Menya, E., Olupot, P.W., Storz, H., Lubwama, M., Kiros, Y., 2018. Characterization and alkaline pretreatment of rice husk varieties in Uganda for potential utilization as precursors in the production of activated carbon and other value-added products. Waste Manag. 81, 104–116.
Menya, E., Olupot, P.W., Storz, H., Lubwama, M., Kiros, Y., John, M.J., 2020. Effect of alkaline pretreatment on the thermal behavior and chemical properties of rice husk varieties in relation to activated carbon production. J. Therm. Anal. Calorim. 139, 1681–1691.
Muthadhi, A., 2010. Studies On Production of Reactive Rice Husk Ash and Performance of RHA Concrete. Pondicherry University, Chennai metropolitan.
Nair, D.G., Fraaij, A., Klaassen, A.A.K., Kentgens, A.P.M., 2008. A structural investigation relating to the pozzolanic activity of rice husk ashes. Cem. Concr. Res. 38, 861–869.
Nath, P., Sarker, P., 2012. Geopolymer concrete for ambient curing condition. In: Proceedings of the Australasian Structural Engineering Conference 2012 (ASEC 2012), July 11–13, 2012, pp. 1–9.
Nuaklong, P., Sata, V., Chindaprasirt, P., 2018. Properties of metakaolin-high calcium fly ash geopolymer concrete containing recycled aggregate from crushed concrete specimens. Constr. Build. Mater. 161, 365–373.
Saloma, H., Debby, O.E., Della, G.M., 2017. Effect of Na_2SiO_3/NaOH on mechanical properties and microstructure of geopolymer mortar using fly ash and rice husk ash as precursor. In: Proceedings of the 3rd International Conference on Construction and Building Engineering (ICONBUILD), 2017.
Singh, B., Ishwarya, G., Gupta, M., Bhattacharyya, S.K., 2015. Geopolymer concrete: a review of some recent developments. Constr. Build. Mater. 85, 78–90.
Singh, N.B., 2018. Fly ash-based geopolymer binder : a future. Minerals 8, 299.
Sore, S.O., Messan, A., Prud'homme, E., Escadeillas, G., Tsobnang, F., 2016. Synthesis and characterization of geopolymer binders based on local materials from Burkina Faso - Metakaolin and rice husk ash. Constr. Build. Mater. 124, 301–311.

Sridhar, G., Sridhar, H.V., Dasappa, S., Paul, P.J., Rajan, N.K.S., Shrinivasa, U., Mukunda, H.S., 1996. Technology for gasifying pulverised bio-fuels including agricultural residues. Energy Sustain. Dev. 3, 9–18.
Subramanian, P., Sampathrajan, A., Venkatachalam, P., 2011. Fluidized bed gasification of select granular biomaterials. Bioresour. Technol. 102, 1914–1920.
Sugita, S., 1993. On the economical production of large quantities of highly reactive rice husk ash. In: International Symposium on Innovative World of Concrete (ICI-IWC-93), pp. 3–71.
Tirawanichakul, S., Tirawanichakul, Y., Sniso, E., 2008. Paddy dehydration by adsorption: thermo-physical properties and diffusion model of agriculture residues. Biosyst. Eng. 99, 249–255.
Tripathi, M., Sahu, J.N., Ganesan, P., 2016. Effect of process parameters on production of biochar from biomass waste through pyrolysis: a review. Renew. Sustain. Energy Rev. 55, 467–481.
UNBS, 2018. Cement—Part 1: composition, specification and conformity criteria for common cements. Uganda National Bureau of Standards, Kampala, Uganda.
Vélez, J.F., Chejne, F., Valdés, C.F., Emery, E.J., Londoño, C.A., 2009. Co-gasification of Colombian coal and biomass in fluidized bed: an experimental study. Fuel 88, 424–430.
Wanyama, I., Ochwoh, V., Nankya, E., Van Asten, J., 2015. Optimization of major nutrients (N, P and K) for lowland rice production in eastern Uganda. Int. J. Agron. Agric. Res. 7, 218–227.
Zareei, S.A., Ameri, F., Dorostkar, F., Ahmadi, M., 2017. Rice husk ash as a partial replacement of cement in high strength concrete containing micro silica: evaluating durability and mechanical properties. Case Stud. Constr. Mater. 7, 73–81.
Zhang, J.R., Liu, G.Y., Chen, B., Song, D., Qi, J., Liu, X.Y., 2014. Analysis of CO_2 emission for the cement manufacturing with alternative raw materials: a LCA-based framework. Energy Procedia 61, 2541–2545.